Valley splitting in Si quantum dots embedded in SiGe

S. Srinivasan,[1,2] G. Klimeck,[1,2] and L. P. Rokhinson[2,3,a]

[1]Network for Computational Nanotechnology, Purdue University, West Lafayette, Indiana 47907, USA
[2]Birck Nanotechnology Center, Purdue University, West Lafayette, Indiana 47907, USA
[3]Department of Physics, Purdue University, West Lafayette, Indiana 47907, USA

We examine energy spectra of Si quantum dots embedded in $Si_{0.75}Ge_{0.25}$ buffers using atomistic numerical calculations for dimensions relevant to qubit implementations. The valley degeneracy of the lowest orbital state is lifted and valley splitting fluctuates with monolayer frequency as a function of the dot thickness. For dot thicknesses ≤ 6 nm, valley splitting is found to be >150 μeV. Using the unique advantage of atomistic calculations, we analyze the effect of buffer disorder on valley splitting. Disorder in the buffer leads to the suppression of valley splitting by a factor of 2.5; the splitting fluctuates with ≈ 20 μeV for different disorder realizations. Through these simulations we can guide future experiments into regions of low device-to-device fluctuations. © 2008 American Institute of Physics. [DOI: 10.1063/1.2981577]

Understanding and design of silicon nanometer-scaled electronic devices have regained significant interest. This interest is sparked by the experimental progress that enabled the reproducible construction of geometries in which electrons are confined in three dimensions (3D) to length scales of a few nanometers and the potential applications of this technology to ultrascaled traditional complementary metal-oxide-semiconductor devices. Emerging application of Si nanostructures for qubit implementations due to long spin relaxation times[1–3] imposes additional stringent requirements on energy spectrum engineering, including the precise control of valley degeneracy. The sixfold valley degeneracy of bulk Si is reduced to twofold degeneracy when electrons are confined to two dimensions (2D) such as at Si/SiO_2 interface in mainstream metal-oxide-semiconductor field-effect transistors. Decades ago it was recognized that there is a small splitting between the two valleys in the lowest subband.[4] Recently, calculations predicted that valley splitting in narrow (few nanometers) SiGe/Si/SiGe quantum wells (QWs) can be of the order of 10–100 meV and should fluctuate rapidly with the well thickness.[5–8] However, experiments[9–11] produced valley splitting about two orders of magnitude smaller than that prediction, which has been explained[12] by the disorders of the Si/SiGe interface and in the SiGe buffer. The experiments[13] and theoretical methods indicated that additional spatial confinement will minimize the role of interface disorder and increase valley splitting. In this paper we investigate the role of SiGe buffer disorder on valley splitting and answer the fundamental question of the size and controllability of valley splitting for relevant experimental structures.

3D confinement of electrons can be achieved by various techniques. Electrostatic surface gating of 2D gas provides relatively weak and smooth spatial confinement potentials. In contrast, 3D confinement by Si/SiO_2 interface produces sharp potential with Coulomb energies approaching room temperature[14,15] and large valley splitting.[16] Recently, an alternative approach to 3D confinement has been demonstrated with an advantage of lithographically defined epitaxial Si/SiGe interfaces using postfabrication regrowth.[17] In this case

spurious charging effects[18] related to the traps in SiO_2 or unpassivated interface can be avoided, yet retaining sharp confining potential. We will simulate such defined Si nanostructures in SiGe buffers and explore sizes relevant for qubit implementations. Simulation capabilities to represent structures containing 10^7 atoms explicitly enable the atomic representation of the dot, interfaces, and the SiGe buffer. Atomistic simulations also present a unique opportunity to vary the amount of the buffer disorder in order to attain detailed understanding of the physics of valley splitting, including its magnitude and fluctuations. The valley splitting is primarily defined by the smallest dimension of the device, and our conclusions are applicable to any Si nanostructure defined from SiGe/Si/SiGe QWs.

Calculations of the energy spectrum are performed using the NEMO-3D general purpose code, which represents each atom in the domain explicitly. The theory underlying the tool and its relevant benchmarks are given in Refs. 19 and 20. The structure is defined on the relaxed (001) $Si_{0.75}Ge_{0.25}$ substrate, and the Keating valence-force field model is used to adjust atomic positions to minimize the strain energy. Calculations of electronic structure are based on the 20 band $sp^3d^5s^*$ tight-binding model. The quantum dot was modeled as a $l_x \times l_y \times l_z$ rectangle grown on 37-nm-thick substrate and embedded in 27-nm-thick $Si_{0.75}Ge_{0.25}$ buffer, $l_z < l_x, l_y$, where z is along the growth direction. We investigated the influence of the buffer thickness on electronic structure; there were no significant changes for substrates $t_s > 30$ nm and buffers $t_b > 20$ nm.

For 25% Ge we can generate various placements of Ge atoms in the $Si_{0.75}Ge_{0.25}$ buffer, with fully ordered containing only Si–Ge bonds, partially ordered containing single Ge–Ge bond per eight-atom supercell in a fixed position, and disordered having random placement of Ge atoms retaining 25% composition (see schematic in Fig. 1).

We start with the analysis of energy levels and valley splitting in a dot embedded in a fully ordered buffer. Evolution of energy levels for a $l_x \times 20 \times 10$ nm^3 dot is shown in Fig. 2 (the actual dot thickness is $l_z = 9.85$ nm $= 72$ ML). All levels come in pairs, both levels in the pair having similar wave function envelopes (each level is also double spin degenerate, which has been confirmed by calculations and will
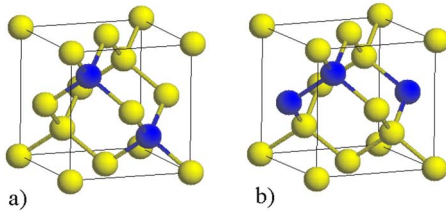
a)Electronic mail: leonid@purdue.edu.

93, 112102-1   © 2008 American Institute of Physics

FIG. 1. (Color online) Placement of Si (yellow, light) and Ge (blue, dark) atoms in (a) fully ordered (Si–Ge and Si–Si bonds) and (b) partially ordered (Si–Ge, Ge–Ge, and Si–Si bonds) eight-atom supercells.

be ignored for the rest of the paper). The 3D representations of the envelope wave functions at 20% value are shown for the lowest six levels. The two lowest levels have similar s-type wave functions and represent the same orbital state with different valley numbers. The energy difference between them we call valley splitting Δ_v^0. The next two levels have one node and belong to the next orbital state. For l_x <25 nm the p_z-type state has lower energy than p_x- and p_y-type states due to the combination of sizes and effective mass anisotropy. The p_x-type level has the highest sensitivity to l_x, as expected, and for $l_x>26$ nm its energy becomes lower than that of the p_z-type state. Energy separation between the ground and the first exited orbital states δE $\approx 8-10$ meV is large enough to restrict qubit Hilbert space to the lowest orbital state at low temperatures.

Valley mixing results from superposition of two counter-propagating waves reflected from the opposite Si/SiGe heterointerfaces of the dot. The phase difference of the two waves depends on the details of the interface. The strength of the mixing depends on the amplitude of the wave functions at the interfaces, $\Delta_v \propto |\chi(l_b)|^2$, where $\chi(l_b)$ is the value of the envelope of the electron wave function at the dot boundary.[7] For p_z-type and d_z-type (top curve in Fig. 2) states, wave functions are pushed toward z-heterointerface, and valley splitting for these states are significantly larger than for the ground and p_x- or p_y-type states.

The most interesting question that can be uniquely studied by atomistic calculations is the role of buffer disorder.
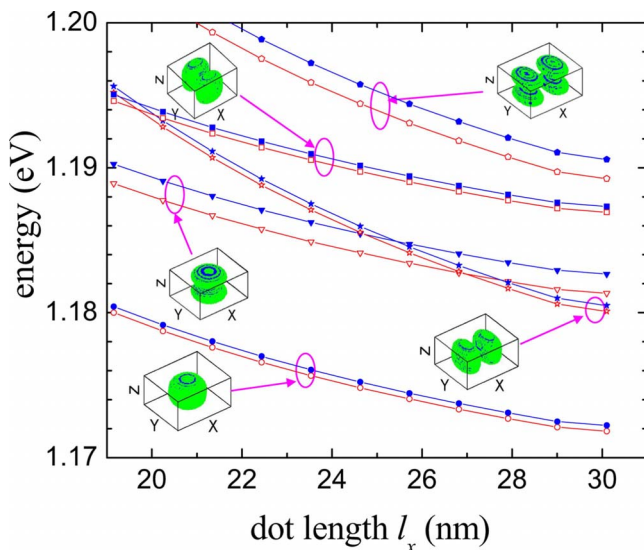

FIG. 2. (Color online) Energy levels in $l_x \times 20 \times 10$ nm³ Si dot embedded in ordered Si$_{0.75}$Ge$_{0.25}$ buffer. Energies are referenced to the valence band Γ_v^8 point. Inserts show spatial distribution of wave functions for the lowest levels.
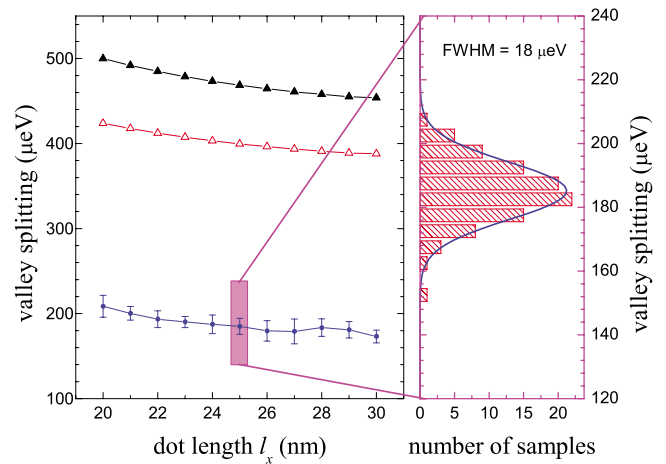

FIG. 3. (Color online) Valley splitting for the lowest orbital level as a function of the dot size for ordered (black), partially ordered (red), and disordered (blue) Si$_{0.75}$Ge$_{0.25}$ buffer. Bars indicate standard deviation for each point. An example of valley splitting distribution for 100 realizations of buffer disorder is shown in the histogram for $l_x=25$ nm; blue curve is the Gaussian fit.

In Fig. 3 valley splitting of the ground level is plotted for a $l_x \times 20 \times 10$ nm³ dot as a function of the dot size l_x for fully ordered, partially ordered, and completely disordered buffer. For fully ordered buffer the valley splitting is ~0.5 meV, consistent with analytical calculations. The value does not change significantly with the dot size, which confirms that valley splitting is primarily determined by the smallest dimension. For partially ordered buffers we see a reduction in Δ_v^0 by 10%, while for fully disordered buffer Δ_v^0 is reduced 2.5 times to ~0.2 meV. To investigate fundamental reproducibility of Δ_v^0, we performed calculations for 100 realizations of the buffer disorder for each point. The histogram of Δ_v^0 for $l_x=25$ nm dot is plotted in the right frame. The distribution is Gaussian, with standard deviation of 9.4 μeV, which is ~5% of Δ_v^0. The bars on the main plot indicate standard deviation for other dot sizes.

Intervalley mixing is very sensitive to the smallest dimension of the dot l_z and fluctuates with a monolayer frequency $\Delta_v \propto \cos(k_0 l_z)$, where $k_0=0.82(2\pi/a)$ is the center of the valleys and a is the lattice constant. Valley splitting as a function of l_z with monolayer resolution is plotted in Fig. 4 (black line), and bars indicate standard deviation for different disorder realizations. The calculated valley splitting fluctuates rapidly with 1 ML period, as emphasized by thin line for low l_z. It has been noted, however, that QWs with odd and even numbers of monolayers belong to different symmetry classes.[7] Indeed, if we connect Δ_v^0 for even and odd numbers of monolayers, we obtain two similar curves, which fluctuate with a period of ≈ 8 ML and are out of phase with each other. The value of $\Delta_v^0(l_z)$ for the dot embedded in a disordered buffer is reduced by a factor of 2.5, as shown in the inset. For comparison we also plot valley splitting calculated for the 2D QW using envelope function method[8] (dashed line), which coincides with our calculations for the ordered buffer. Saturation of valley splitting for large l_z, compared with the $1/l_z^3$ analytical dependence, is due to an additional lateral confinement. In the inset of Fig. 4 stars indicate percentage of the wave function $|\chi(z)|^2$, which penetrates the buffer above and below the dot; the envelope of Δ_v^0 follows $|\chi(z)|^2$ as a function of l_z.
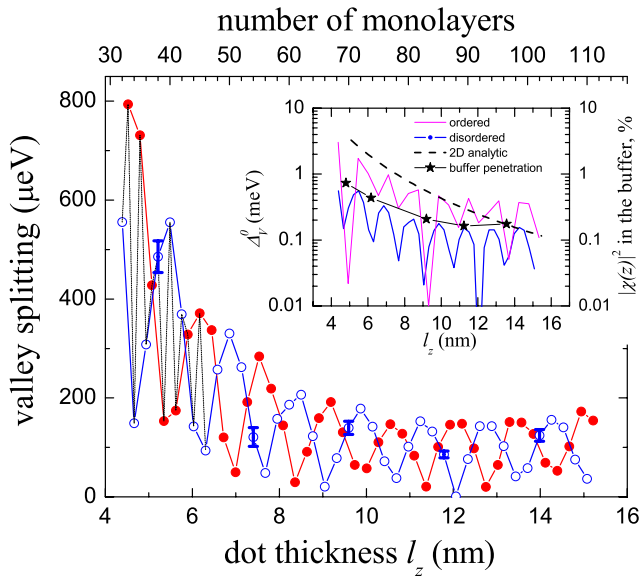
FIG. 4. (Color online) Valley splitting for the lowest orbital level of $25 \times 20 \times l_z$ nm^3 Si dot as a function of the dot thickness in monolayers. l_z is calculated using 1 ML ≈ 0.13707 nm. Thin line connects points with 1 ML step, thick lines connect points for even (open dots) and odd (solid dots) monolayers. Bars indicate standard deviations for different disorder realizations. In the inset Δ_v^0 for ordered and disordered buffers are plotted. Dashed line is Δ_v^0 obtained analytically for the 2D case. Stars show percent of the wave function penetrating into the buffer in z-direction (right scale).

To summarize, we calculate energy levels and valley splitting for a small Si dot embedded in a disordered Si$_{0.75}$Ge$_{0.25}$ buffer. We find that buffer disorder leads to the suppression of valley splitting by ~ 2.5 and actual values fluctuate with standard deviation of ~ 20 μeV. At the same time disorder limits the lowest valley splitting, which can reach zero for a perfectly ordered buffer for some dot thicknesses, and dots with valley splitting of >150 μeV can be predictably designed from narrow QW ($l_z \leq 6$ nm).

[1] B. Kane, Nature (London) **393**, 133 (1998).

[2] Z. Wilamowski, W. Jantsch, H. Malissa, and U. Rössler, Phys. Rev. B **66**, 195315 (2002).

[3] A. Tyryshkin, S. Lyon, W. Jantsch, and F. Schäffler, Phys. Rev. Lett. **94**, 126802 (2005).

[4] T. Ando, A. B. Fowler, and F. Stern, Rev. Mod. Phys. **54**, 437 (1982).

[5] T. B. Boykin, G. Klimeck, M. A. Eriksson, M. Friesen, S. N. Coppersmith, P. von Allmen, F. Oyafuso, and S. Lee, Appl. Phys. Lett. **84**, 115 (2004).

[6] T. B. Boykin, G. Klimeck, M. Friesen, S. N. Coppersmith, P. von Allmen, F. Oyafuso, and S. Lee, Phys. Rev. B **70**, 165325 (2004).

[7] M. O. Nestoklon, L. E. Golub, and E. L. Ivchenko, Phys. Rev. B **73**, 235334 (2006).

[8] M. Friesen, S. Chutia, C. Tahan, and S. N. Coppersmith, Phys. Rev. B **75**, 115318 (2007).

[9] P. Weitz, R. Hauga, K. V. Klitzing, and F. Schäffler, Surf. Sci. **361**, 542 (1996).

[10] S. Koester, K. Ismail, and J. Chu, Semicond. Sci. Technol. **12**, 384 (1997).

[11] K. Lai, W. Pan, D. C. Tsui, S. Lyon, M. Mühlberger, and F. Schäffler, Phys. Rev. Lett. **93**, 156805 (2004).

[12] N. Kharche, M. Prada, T. B. Boykin, and G. Klimeck, Appl. Phys. Lett. **90**, 092109 (2007).

[13] S. Goswami, K. Slinker, M. Friesen, L. McGuire, J. Truitt, C. Tahan, L. Klein, J. Chu, P. Mooney, D. V. der Weide, R. Joynt, S. Coppersmith, and M. Eriksson, Nat. Phys. **3**, 41 (2007).

[14] Y. Takahashi, M. Nagase, H. Namatsu, K. Kurihara, K. Iwdate, Y. Nakajima, S. Horiguchi, K. Murase, and M. Tabe, Electron. Lett. **31**, 136 (1995).

[15] L. Zhuang, L. Guo, and S. Y. Chou, Appl. Phys. Lett. **72**, 1205 (1998).

[16] L. P. Rokhinson, D. C. Tsui, L. N. Pfeiffer, and K. W. West, Superlattices Microstruct. **32**, 99 (2002).

[17] X.-Z. Bo, L. Rokhinson, N. Yao, D. Tsui, and J. Sturm, J. Appl. Phys. **100**, 094317 (2006).

[18] L. P. Rokhinson, L. J. Guo, S. Y. Chou, and D. C. Tsui, Appl. Phys. Lett. **76**, 1591 (2000).

[19] G. Klimeck, F. Oyafuso, T. Boykin, R. Bowen, and P. von Allmen, Comput. Model. Eng. Sci. **3**, 601 (2002).

[20] G. Klimeck, S. Ahmed, H. Bae, N. Kharche, S. Clark, B. Haley, S. Lee, M. Naumov, H. Ryu, F. Saied, M. Prada, M. Korkusinski, T. Boykin, and R. Rahman, IEEE Trans. Electron Devices **54**, 2079 (2007).